



저작자표시-비영리-변경금지 2.0 대한민국

이용자는 아래의 조건을 따르는 경우에 한하여 자유롭게

- 이 저작물을 복제, 배포, 전송, 전시, 공연 및 방송할 수 있습니다.

다음과 같은 조건을 따라야 합니다:



저작자표시. 귀하는 원저작자를 표시하여야 합니다.



비영리. 귀하는 이 저작물을 영리 목적으로 이용할 수 없습니다.



변경금지. 귀하는 이 저작물을 개작, 변형 또는 가공할 수 없습니다.

- 귀하는, 이 저작물의 재이용이나 배포의 경우, 이 저작물에 적용된 이용허락조건을 명확하게 나타내어야 합니다.
- 저작권자로부터 별도의 허가를 받으면 이러한 조건들은 적용되지 않습니다.

저작권법에 따른 이용자의 권리는 위의 내용에 의하여 영향을 받지 않습니다.

이것은 [이용허락규약\(Legal Code\)](#)을 이해하기 쉽게 요약한 것입니다.

[Disclaimer](#)

Degree Thesis for M. Eng.

**Analysis on Statistical Characteristics of Partial Discharges
in SF₆ Gas under HVDC**



August 2015

Department of Electrical and Electronics Engineering

The Graduate School of Korea Maritime and Ocean University

Guoming Wang

**Thesis submitted by Guoming Wang in fulfillment
of requirement for the degree of M. Eng.**

Committee Chairman : D. Eng. Yoon-Sik Kim (印)

Committee Member : D. Eng. Gyung-Suk Kil (印)

Committee Member : D. Eng. Nakwon Jang (印)

June 2015

Department of Electrical and Electronics Engineering

The Graduate School of Korea Maritime and Ocean University

Guoming Wang

Contents

Contents	i
Lists of Figures and Table	iii
Abstract	v
Chapter 1 Introduction	1
Chapter 2 Theory	3
2.1 Partial discharge	3
2.2 Detection and analysis methods	9
2.2.1 Detection methods	10
2.2.2 Analysis methods	14
Chapter 3 Experiment and Analysis	18
3.1 Experiment	18
3.1.1 Insulation defects	18
3.1.2 Measurement system	21
3.1.3 Experimental setup	23
3.2 Results and Analysis	24

3.2.1 DIV and DEV	24
3.2.2 Discharge magnitude and pulse count	27
3.2.3 Statistical characteristics	30
Chapter 4 Conclusions	39
References	41



Lists of Figures and Table

<List of Figures>

Fig. 1.1 HVDC transmission systems around the world	2
Fig. 2.1 Equivalent circuit of internal discharge under AC	4
Fig. 2.2 Recurrence of discharge	5
Fig. 2.3 Equivalent circuit of internal discharge under DC	8
Fig. 2.4 Voltage across a cavity in a solid dielectric under DC	8
Fig. 2.5 Series PD test circuit	10
Fig. 2.6 AE signal and its EC curve	11
Fig. 2.7 UHF sensors	12
Fig. 2.8 Example of PRPD detected by electrical method	14
Fig. 2.9 PD sequence	16
Fig. 3.1 Electrode systems	20
Fig. 3.2 Blockdiagram of measurement system	21
Fig. 3.3 Blockdiagram of RT VI	22
Fig. 3.4 Experimental setup	23
Fig. 3.5 DIV and DEV as a function of gas pressure	26
Fig. 3.6 Discharge magnitude and pulse count as a function of applied voltage ..	30
Fig. 3.7 Discharge distribution and density function of POC	32
Fig. 3.8 Discharge distribution and density function of POE	33
Fig. 3.9 Discharge distribution and density function of FP	34
Fig. 3.10 Discharge distribution and density function of Void	35
Fig. 3.11 Discharge distribution and density function of Crack	36
Fig. 3.12 Distribution of statistical characteristics	38

<List of Table>

Table 2.1 DGA interpretation 13



**Analysis on Statistical Characteristics of Partial Discharges
in SF₆ Gas under HVDC**

by Guoming Wang

Department of Electrical and Electronics Engineering
The Graduate School of Korea Maritime and Ocean University
Busan, Republic of Korea

Abstract

With the rapid development of HVDC technology and the issue of smart grid, it is a new challenge to monitor and diagnose performance of the related power facilities. This thesis dealt with the statistical characteristics of partial discharge (PD) pulse in SF₆ gas under HVDC in terms of discharge inception voltage (DIV) and discharge extinction voltage (DEV), discharge magnitude, and pulse count as well as the statistical characteristics extracted from the discharge distribution and density function.

To simulate the typical insulation defects in gas insulated switchgear (GIS), electrode systems such as a protrusion on conductor (POC), a protrusion on enclosure (POE), a free particle (FP), a void inside spacer (Void), and a crack inside spacer (Crack) were fabricated. All of them were filled with SF₆ gas in ranges from 0.1 MPa to 0.5 MPa. A HVDC source

was generated by a rectifying circuit which is composed of a 100 kV diode, and a 0.5 μ F capacitor. PD signal produced from the electrode systems was detected through a 50 Ω non-inductive resistor and was analyzed by a digital storage oscilloscope (DSO) with a sampling rate of 5 GS/s and a DAQ system based on LabVIEW program.

The DIV and DEV in POC, POE, and Crack increased with the gas pressure. The gas pressure did not strongly affect the DIV and DEV in FP. The DIV and DEV in Void were almost similar to the increase of the SF₆ gas pressure. The maximum discharge magnitude Q_{max} and pulse count in 5 seconds of each electrode system increased as the applied voltage was raised. However, the mean discharge magnitude Q_{mean} did not change significantly. For each electrode system, the discharge distribution and density function presented distinguishable patterns. Therefore, it is possible to identify the type of defects in gas insulated equipment operated under HVDC by analysing statistical characteristics extracted from the discharge distribution and density function.

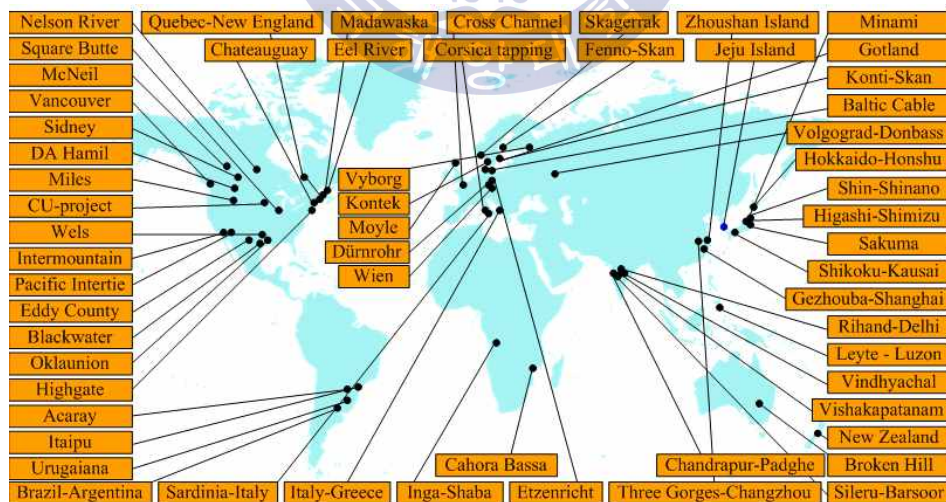
Chapter 1 Introduction

With the development of high voltage valves, the high voltage direct current (HVDC) transmission has been applied in the electricity industry for 60 years since the first HVDC system was commissioned in Gotland in 1954. As the result of advantages of asynchronous interconnections, lower investment, environmental concerns, and long distance transmission, there are increasing demands for HVDC solution, which is expected to double within the next five years from a current 2.8 billion dollars per year. Fig. 1.1 shows the HVDC transmission systems that have been installed around the world. In Korea, the first HVDC project was commercially operated to link Jeju Island with the mainland via a submarine connection of 300 MW and 101 km in 1998. In 2012, Jeju #2 project with 400 MW was finally completed and Jeju #3 project is to be completed by 2018. Also the large scale off-shore project in West Sea and metropolitan project for enhancement of the system reliability are under consideration^{[1],[2]}.

The gas insulated power equipment such as gas insulated switchgear (GIS) and gas insulated transmission line (GIL) play important roles in HVDC distribution and transmission. However, failures of such power facilities caused by electrical, thermal, mechanical, and environmental stress lead to considerable financial loss and personal injure. It is therefore essential to diagnose their condition to ensure the reliable operation of power system especially under the background of smart grid. Due to the availability of sensors and computer aided signal processing technology, the diagnostic

technique have been promoted from classical off-line method to on-line monitoring. The partial discharge (PD), which is regarded as the initial stage of deterioration, has been researched a lot under AC voltage for insulation evaluation of power apparatus. Up to now, the PD under DC voltage has not been investigated in detail and the experience from AC PD measurements can not be applied to DC directly. Therefore, it is necessary to study PD behavior under DC voltage for condition monitoring of HVDC equipment^[3].

This thesis dealt with the PD characteristics in SF₆ gas under HVDC. Typical insulation defects were fabricated to simulation PD sources in GIS. The discharge inception and extinction voltage as a function of gas pressure, discharge magnitude and pulse count as a function of applied voltage as well as the statistical characteristics of discharge distribution and density function were analyzed.



Ref. : Roberto Rudervall et al, "High Voltage Direct Current (HVDC) Transmission Systems Technology Review Paper"

Fig. 1.1 HVDC transmission systems around the world

Chapter 2 Theory

2.1 Partial discharge

Gases are the simplest and the most widely used dielectrics in the insulation system of power facilities. The initial physical process of gas discharge is called ionization, which means separation an electron from an atom or a molecule in case the atom or the molecule achieves the ionization energy from collision, photon, thermal energy or cathode processes. Once a free electron is available in the gas, it is accelerated in the direction of electric field and leads to avalanches, making further ionization of other atom or molecule. The positive ions generated in the avalanche process are also accelerated by the applied field towards the cathode and self-sustaining discharge occurs if sufficient secondary electrons are released from the cathode. These are called Townsend mechanism and explain breakdown phenomena only at low gas pressure and short distance between two electrodes. For a large pressure-distance value, usually the streamer theory is applied. The Streamer mechanism emphasizes that the distortion of electric field due to the space charge and the photons created by recombination affect the ionization process^[4].

The PD is defined as a localized electrical discharge that only partially bridges the insulation between conductors and which can or cannot occur adjacent to a conductor. PD activity can occur at any point in the insulation system, where the electric field strength exceeds the breakdown strength of that portion of the insulating material. Although the magnitude of such

discharge is usually small at its early stage, it causes progressive deterioration and finally results in the failure of power apparatus such as power transformer, GIS, and GIL. It is therefore essential to detect PD for condition monitoring and diagnosis of the insulation system^{[5],[6]}.

Fig. 2.1 shows the well-known *a-b-c* circuit which describes the behaviour of internal discharge inside a solid or liquid dielectric under AC voltage. Capacitance C_c represents the capacity of the cavity where the discharge occurs, the capacity of the dielectric in series with the cavity is represented by capacitance C_b and the sound part of the dielectric is represented by capacitance C_a . In Fig. 2.1, the faulty part of the dielectric corresponds to I and II is the sound part.

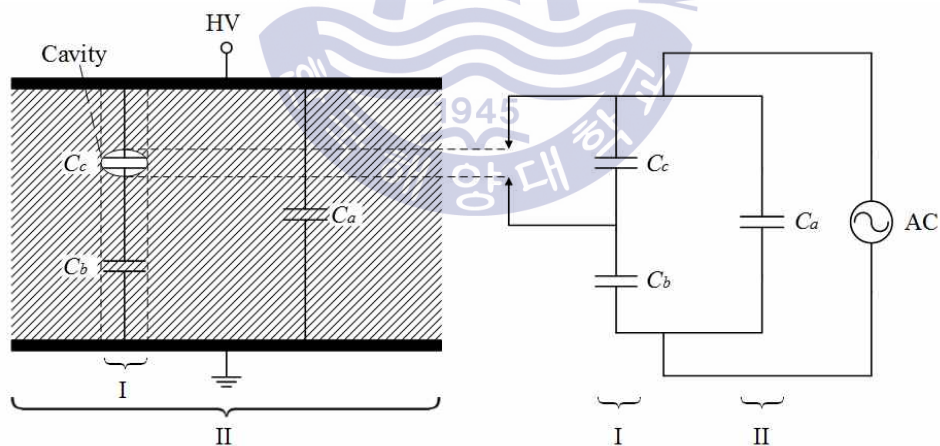


Fig. 2.1 Equivalent circuit of internal discharge under AC

The total capacitance in this circuit is equal to:

$$C = C_a + \frac{C_b C_c}{C_b + C_c} \quad (2.1)$$

If AC voltage $V_a = V_m \sin \omega t$ is applied to this sample, the voltage across the cavity V_c is equal to:

$$V_c = \frac{C_b}{C_b + C_c} V_m \sin \omega t \quad (2.2)$$

which is shown in dotted line in Fig. 2.2. When voltage V_c reaches voltage U^+ , which is called partial discharge inception voltage (DIV), a discharge occurs in the cavity. As a result of the opposite field induced by space charge, voltage V_c drops to V^+ at which the discharge extinguishes, this voltage is called partial discharge extinction voltage (DEV).

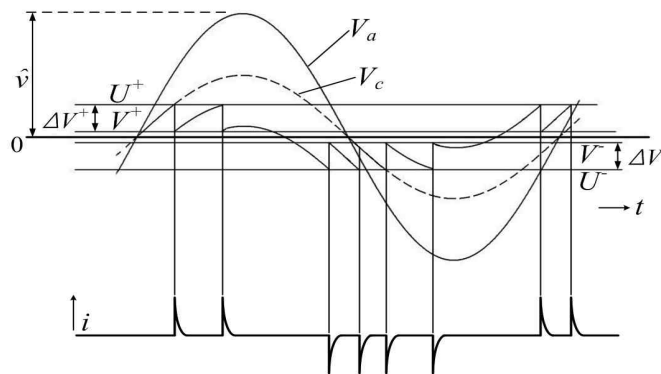


Fig. 2.2 Recurrence of discharge

A discharge finishes in the cavity and causes a current impulse. This process takes place in less than 10^{-7} s, so the current impulse appears a vertical line in corresponding phase. As the applied voltage increases, discharge recurs when V_c reaches U^+ again. The same phenomenon occurs at the negative half of the applied voltage.

Transfer charge q_t which is released from the cavity is equal to:

$$q_t = \left(C_c + \frac{C_a C_b}{C_a + C_b}\right)(U - V) = \left(C_c + \frac{C_a C_b}{C_a + C_b}\right)\Delta V \quad (2.3)$$

while $C_a \gg C_b$, thus

$$q_t = (C_b + C_c)\Delta V \quad (2.4)$$

However, q_t can not be measured and it is therefore not a practical choice to evaluate PD.

The voltage drop ΔV caused by discharge distributes inversely with capacitance C_a and C_b , the voltage drop in capacitance C_a is equal to:

$$\Delta V_a = \frac{C_b}{C_a + C_b} \Delta V \quad (2.5)$$

which means that, when discharge occurs in the cavity, there will be a voltage drop in the sample and corresponding charge q will be released from the test object:

$$q = (C_a + C_b)\Delta V_a = C_b\Delta V \quad (2.6)$$

The discharge magnitude q is defined as apparent charge, which is an important parameter for evaluation of PD and usually expressed in picocoulomb (pC). According to IEC 60270, the apparent charge q of a PD pulse is the charge which, if injected within a very short time between the terminals of the test object in a specified test circuit, would give the same reading on the measurement instrument as the PD current pulse itself. The measurement of apparent charge is carried out by calibration process which is made to determine the scale factor k .

By comparing equation 2.4 with 2.6, the ratio of q to q_t is given by:

$$\frac{q}{q_t} = \frac{C_b}{C_b + C_c} \quad (2.7)$$

it verifies the proportional relation between apparent discharge and transfer discharge and q can be used as a measure for discharge^{[7],[8]}.

Different from that under high voltage AC, as a result of absence of change both in amplitude and polarity of the DC voltage, once PD occurs in the cavity, the opposite field induced by space charge makes PD extinguish. Discharge will recur until the induced field decreases to some degree due to the dissipation of space charge through the dielectric conductivity. In other words, the space charge disappears in the form of leakage current. Based on above consideration, the equivalent circuit for internal discharge under DC is

presented by the a-b-c model extended with some resistive elements in parallel with the corresponding capacitances, which is shown in Fig. 2.3. C_c and R_c represent the cavity, C_b and R_b represent the property of the sound part in series with the cavity, C_a and R_a represent the property of the rest part.

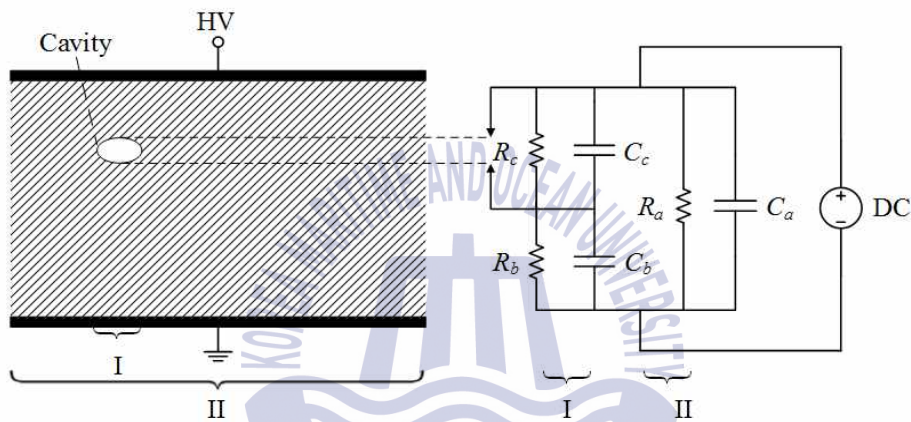


Fig. 2.3 Equivalent circuit of internal discharge under DC

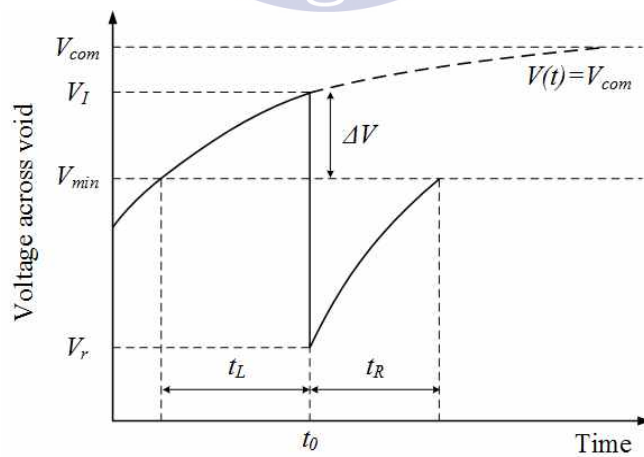


Fig. 2.4 Voltage across a cavity in a solid dielectric under DC

The voltage across a cavity in a solid dielectric under DC is shown in Fig. 2.4. For PD occurrence, two conditions must be satisfied: a initiatory electron and a sufficient electric field. The initiatory electron may come from external environment such as radiation and field emission or from previous discharge. Since the acquirement of initiatory electrons is a stochastic process, statistical time lag t_L is needed, during which the voltage across the cavity increases from the minimum breakdown voltage V_{min} to the DIV. A discharge occurs at t_0 and then drops voltage across the cavity to the residual value V_r . For recurrence of PD, recovery time t_R is required, during which the voltage across the cavity increases from V_r to V_{min} . The time interval Δt between two successive PD is the sum of t_L and t_R ^{[9]-[11]}.

2.2 Detection and analysis methods

With the development of sensors and computer aided data acquisition technology, the condition based maintenance (CBM) based on the continuous on-line monitoring has become the most modern and popular technique for asset management. Regarded as a powerful tool for evaluation of the insulation performance and condition monitoring of the power facilities, PD has been studied in the aspects of detection, analysis, identification, and localization. Based on the different phenomenon generated by PD such as current result from the movement of charges, emission of sound wave and electromagnetic radiation due to the acceleration and deceleration of space charges, as well as the chemical reaction, detection methods can be classified into electrical method complying with IEC 60270 and non-electrical methods including the acoustic emission (AE) method, the ultra high frequency (UHF) method, and the chemical method^{[12],[13]}.

2.2.1 Detection methods

1) Electrical method

The electrical method based on the current flowing in the test circuit is suitable for quantitative measurement of PD in the form of apparent charge. The calibration procedure should be carried out by injecting current pulses with known charge magnitude into the terminal of the test object. There are three typical test circuits for the electrical discharge detection depending the connection manner of the coupling capacitor and the detection impedance: series circuit, parallel circuit, and balanced circuit. The series test circuit is shown in Fig. 2.5, which consists of test object C_a , coupling capacitor C_k to separate PD current from the power current, a detection impedance, a amplifier, and measurement instruments^[5]. According to this method, PD analysis methods such as phase resolved partial discharge (PRPD), time frequency (TF) map, and time resolved partial discharge (TRPD) can be established for the defects identification and the condition assesment of power facilities.

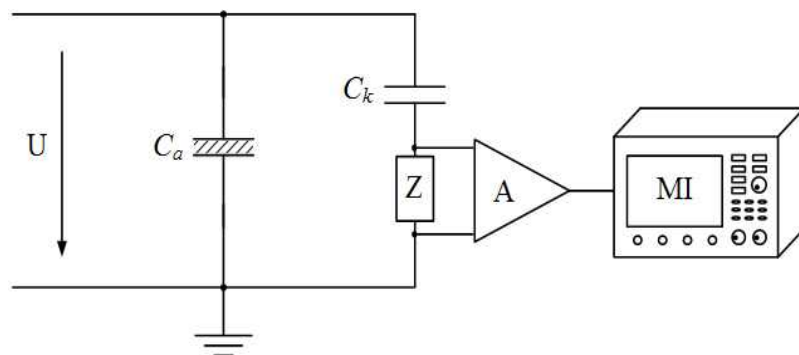


Fig. 2.5 Series PD test circuit

2) Non-electrical methods

A. AE method

When PD occurs, the ultrasonic wave is generated in frequency ranges from 20 kHz to 500 kHz, which can be detected by the AE sensor mounted on the outside of transformer tank or GIS chamber. Since the acoustic signal transmits in all direction from the PD source, the piezoelectric element of sensor can respond to this signal and transduce it into electrical signal. The localization of PD can be carried out by all-acoustic method and electrical-acoustic method. The peak detection, energy criterion (EC), and cross correlation method are recommended to determine the time of arrival. The AE method has the advantages of convenience of use, non-invasive and immune to the electromagnetic noise while it has the disadvantage of signal attenuation, which can be compensated by applying the preamplifier^{[14],[15]}. Fig. 2.6 shows an AE signal and its corresponding EC curve.

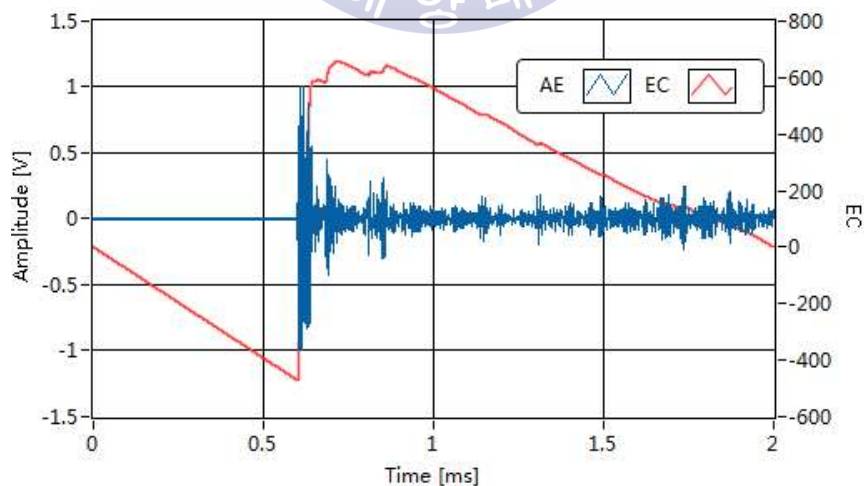


Fig. 2.6 AE signal and its EC curve

B. UHF method

The UHF (300 MHz ~ 3 GHz) method shows obvious advantages such as high sensitivity, robustness to external noise as well as the possibility of on-line monitoring, and is widely applied for PD detection, identification and localization. Generally, the UHF sensors can be classified into internal sensors such as valve sensor for power transformer, internal coupler for GIS and external sensors, for instance, the barrier sensor and window sensor for GIS. Sensors must have a broadband response to cover all frequency contents of PD UHF signal. The background noise including digital video broadcasting (470 MHz ~ 800 MHz) and mobile telephone (800 MHz ~ 2300 MHz) should be taken into consideration when the UHF method is used. The wavelet method is suggested to eliminate interference at specified frequency for the enhancement of the accuracy of measured spectrum. The attenuation and sensitivity check are also important parts for UHF method^{[16],[17]}. Fig. 2.7 shows a valve sensor for power transformer and a window sensor for GIS.



(a) Valve sensor for power transformer

(b) Window sensor for GIS

Ref: Omicron (left), Doble (right)

Fig. 2.7 UHF sensors

C. Chemical method

When the electrical or abnormal thermal faults occur in oil- or gas-insulated apparatus, gases such as H₂, CH₄, C₂H₂, C₂H₄, C₂H₆, and etc. will be produced from the decomposition of insulation material. The dissolved gas analysis (DGA) in accordance with IEC 60599 and IEEE C57.104 is a popular diagnostic method for oil-immersed transformers, which is possible to identify the abnormal conditions by the detected gas ratio. Table 2.1 gives the DGA interpretation recommended in IEC 60599. The types of faults such as PD, discharge of low energy, discharge of high energy, and thermal faults can be distinguished by the analysis of three basic gas ratios. Three other ratios including the CO₂/CO ratio, the O₂/N₂ ratio, and the C₂H₂/H₂ ratio can be used to complement the basic ratios^[18].

Table 2.1 DGA interpretation

Case	Characteristic fault	$\frac{C_2H_2}{C_2H_4}$	$\frac{CH_4}{H_2}$	$\frac{C_2H_4}{C_2H_6}$
PD	Partial discharge	NS	< 0.1	< 0.2
D1	Discharge of low energy	> 1	0.1 ~ 0.5	> 1
D2	Discharge of high energy	0.6 ~ 2.5	0.1 ~ 1	> 2
T1	Thermal fault t < 300 °C	NS	> 1 but NS	< 1
T2	Thermal fault 300 °C < t < 700 °C	< 0.1	> 1	1 ~ 4
T3	Thermal fault t > 700 °C	< 0.2	> 1	> 4

NS : Non-significant whatever the value

2.2.2 Analysis methods

1) PRPD

The PRPD method is an accumulation of the PD data within a certain time including the phase on which discharge occurs, discharge magnitude, and number of discharge, which is also called Φ - q - n pattern. This method is unavailable under DC because of the absence of phase. The PD data can be acquired by the electrical or UHF method. For PD data acquisition, the single sampling time (ST) should be equal to the period of applied AC voltage, the relation between the sampling rate (SR) and the record length (RL) is therefore given by:

$$RL = SR \cdot ST = \frac{SR}{60} \quad (2.8)$$

Fig. 2.8 illustrates an example of PRPD detected by electrical method.

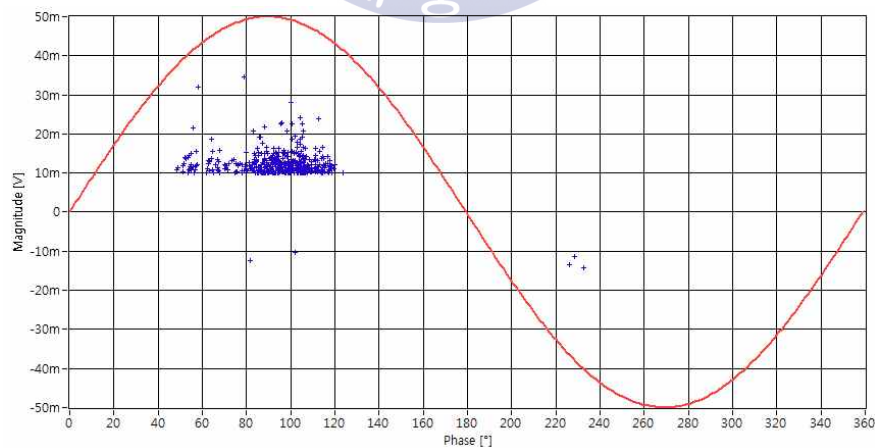


Fig. 2.8 Example of PRPD detected by electrical method

2) TF

The TF method is an analysis of PD in time and frequency domain by extracting the equivalent time σ_T and the equivalent frequency σ_F from each PD pulse. The detected signal $s(t)$ is normalized by:

$$\tilde{s}(t) = \frac{s(t)}{\sqrt{\int_0^T s(t)^2 dt}} \quad (2.9)$$

σ_T and σ_F are the standard deviations which mean the effective range of time around the time gravity and the effective range of the bandwidth around the frequency gravity, respectively and given by:

$$\sigma_T = \sqrt{\int_0^T (t-t_0)^2 \tilde{s}(t)^2 dt} \quad (2.10)$$

$$\sigma_F = \sqrt{\int_0^\infty f^2 |\tilde{S}(f)|^2 df} \quad (2.11)$$

where $\tilde{S}(f)$ is the Fourier transform of the normalized signal, t_0 is the time gravity of $\tilde{s}(t)$ and given by:

$$t_0 = \int_0^T t \tilde{s}(t)^2 dt \quad (2.12)$$

Based on the above analysis, the TF map can be established. The TF map provides method for separation of PD signal from the noise and for PD identification^[19].

3) TRPD and statistical characteristics

In this thesis, the method based on TRPD was used to investigate the statistical characteristics of PD under HVDC. The TRPD is a time-based discharge analysis method based on the PD sequence and it includes two basic quantities: discharge magnitude q_i and time of discharge occurrence t_i . The derived quantity named time interval Δt between two consecutive discharges is important since it is related to the discharge recurrence mechanism.

Fig. 2.9 demonstrates the PD sequence. The measured quantities are time-based discharge sequence (q_i, t_i) , $i=1, 2, 3 \dots N$ and N is the record length of acquisition data. Δt is the time interval between two consecutive discharges. $\Delta t_{pre}=t_i-t_{i-1}$ and $\Delta t_{suc}=t_{i+1}-t_i$ are the time intervals of q_i to its preceding discharge and successive discharge, respectively. Based on the basic quantities and derived quantity, the discharge distribution and density function can be established: PD magnitude as a function of time $q(t)$ which

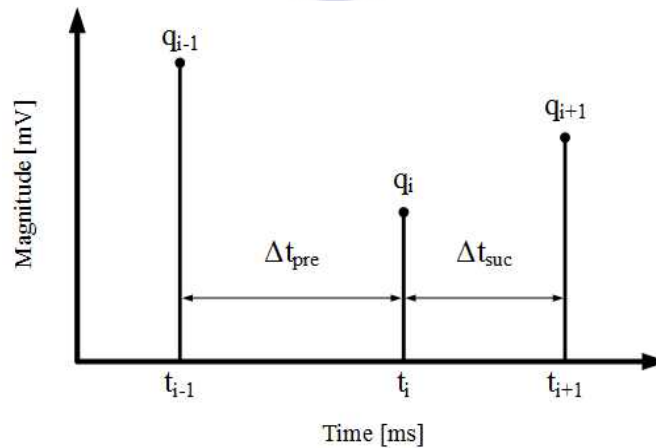


Fig. 2.9 PD sequence

is also called as TRPD, relation between discharge magnitude and time interval to its preceding discharge $q(\Delta t_{pre})$, relation between discharge magnitude and time interval to its successive discharge $q(\Delta t_{suc})$, density function of the discharge magnitude $H(q)$, and density function of the time interval $H(\Delta t)$. Three parameters such as skewness, kurtosis, and peak were used to describe the statistical characteristics of discharge distribution and density function^{[20]-[26]}.

Skewness is a measure of symmetry of a distribution around the sample and defined as:

$$S = \frac{\sum_{i=1}^n (x_i - \mu)^3}{n \cdot \sigma^3} \quad (2.13)$$

where μ is the mean and σ is the standard deviation. Negative values for the skewness indicate data are skewed left and positive values for the skewness indicate data are skewed right. Symmetric data which are called normal distribution have a skewness value of zero.

Kurtosis is an indicator for the steepness of a probability distribution and defined as:

$$K = \frac{\sum_{i=1}^n (x_i - \mu)^4}{n \cdot \sigma^4} \quad (2.14)$$

The normal distribution has a kurtosis value of 3. Data with kurtosis higher than 3 tend to a steep distribution while data with kurtosis lower than 3 tend to distribute evenly.

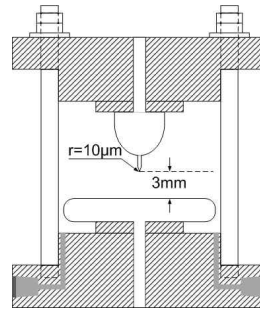
Chapter 3 Experiment and Analysis

3.1 Experiment

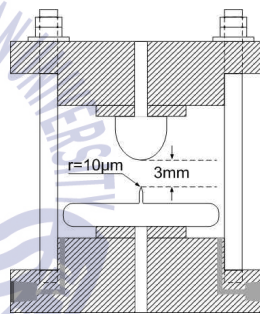
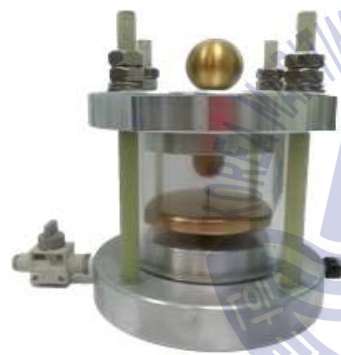
3.1.1 Insulation defects

The PD is generated from the insulation defects of the power equipment due to the electrical stress concentration in the insulation or on the surface of the insulation. The insulation defects may be caused in the manufacture, assembly, transportation, and operation procedure. The defects have different types and therefore result in different discharge patterns and different risk levels. To simulate the typical insulation defects in GIS, five types of electrode systems such as a protrusion on conductor (POC), a protrusion on enclosure (POE), a free particle (FP), a void inside spacer (Void), and a crack inside spacer (Crack) were fabricated. Photographs and schematics are illustrated in Fig. 3.1.

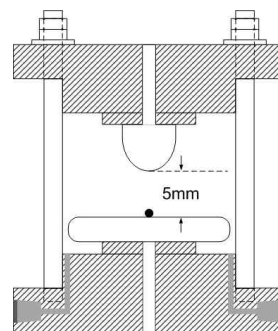
In POC and POE, the curvature radius of the needle was 10 μm and the plane electrode was made of tungsten copper alloy with a diameter of 80 mm and a thickness of 20 mm. To prevent the concentration of electric field, the edge of plane electrode was rounded. The distance between needle and plane electrode was 3 mm. The FP made by a 1 mm-diameter aluminum sphere was placed between two plane electrodes. It was used to simulate the free moving metal in the GIS chamber. The Void was made of epoxy insulator with a cavity. And the Crack was fabricated to simulate a impacted epoxy spacer. The diameter and thickness of the epoxy insulator were 80 mm and 5 mm, respectively.



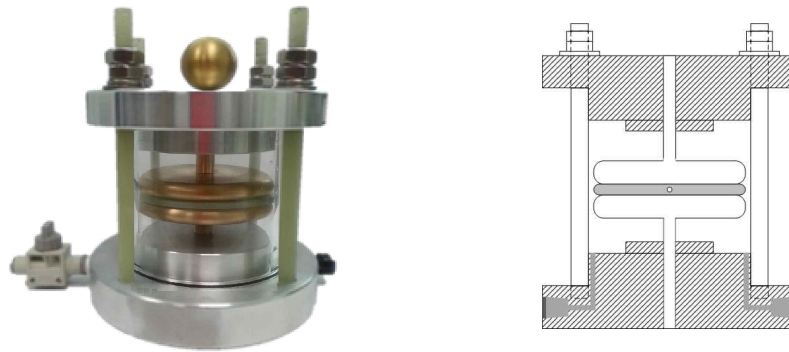
(a) POC



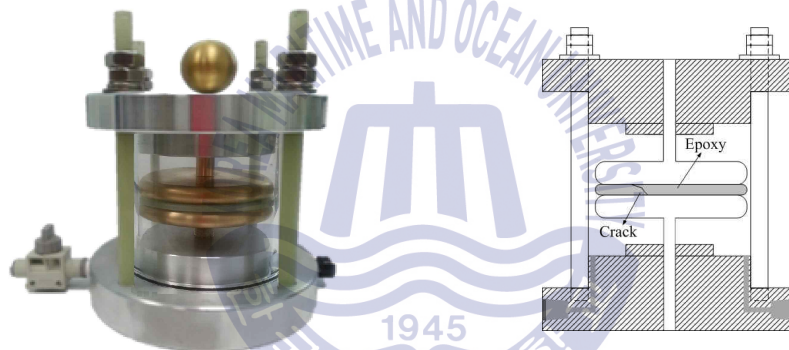
(b) POE



(c) FP



(d) Void



(e) Crack

Fig. 3.1 Electrode systems

3.1.2 Measurement system

The measurement system was developed based on real time operation system (RTOS) by LabVIEW, which is able to run the applications with very precise timing and high degree of reliability. The virtual instrument (VI) in LabVIEW Project Explorer were categorized into two parts by the hardware platform that they will run on: the HOST VI running on the general-purpose computer and the RT VI running on the NI PXI. All of the VI were developed on PC and then connected to the NI PXI via Ethernet to download and run the RT VI. The shared variables were used for command and data communication between two platforms. The blockdiagram of measurement system is shown in Fig. 3.2.

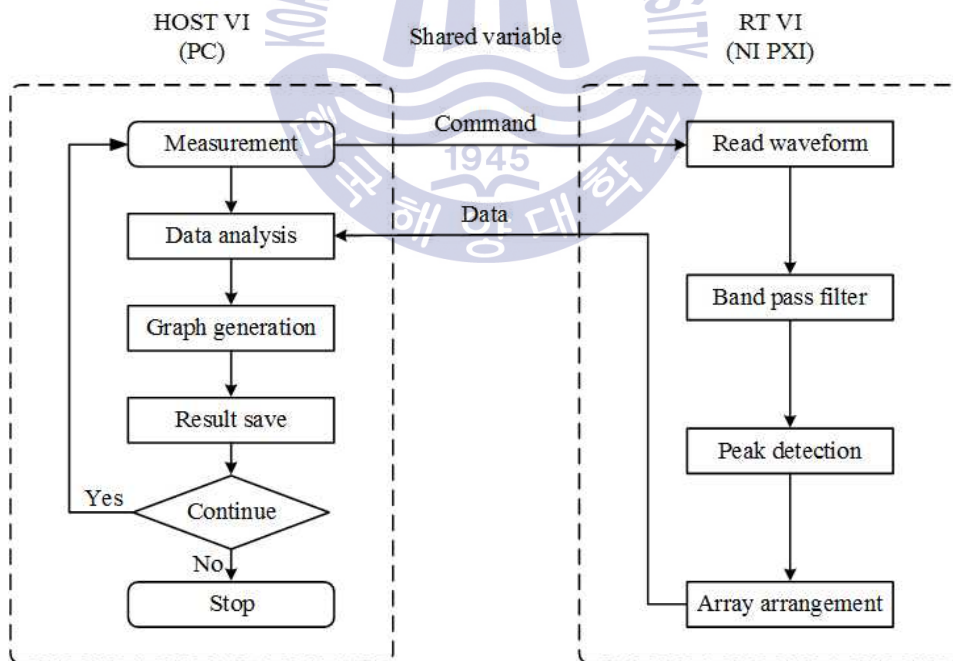


Fig. 3.2 Blockdiagram of measurement system

In the HOST VI, the standard state machine design pattern was built, which allows distinct states to operate in programmatically determined dynamic sequence. It consisted of four states: data analysis, graph generation, results save, and standby. The RT VI included four parts as shown in Fig. 3.3: (1) read waveform from digitizer, (2) software band pass filter, (3) peak detection, and (4) array arrangement. The multi fetch more than available memory and producer-consumer design pattern based on queue operation were used in RT VI. For communication between two platforms, two shared variables were designed. One was used to send commands such as digitizer setting, threshold for peak detection, and configuration of the filter from PC to PXI while another was used to send data from PXI to PC. By applying this proposed system, PD pulse can be measured and analyzed in real time within a specified period.

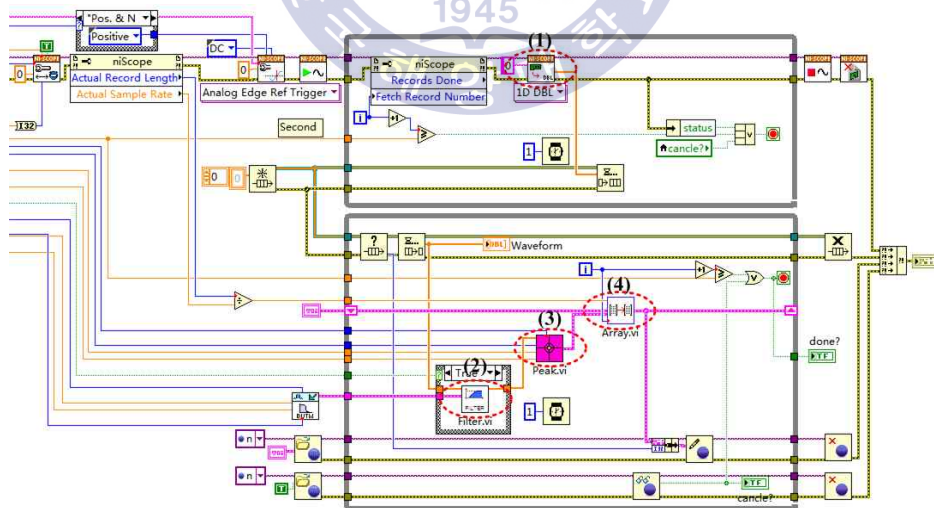


Fig. 3.3 Blockdiagram of RT VI

3.1.3 Experimental setup

The experimental setup is demonstrated in Fig. 3.4. A HVDC source was generated by a rectifying circuit which is composed of a transformer, a 100 kV diode, and a 0.5 μ F capacitor. For limiting the current, a resistor R was used in the test circuit. Electrode systems filled with SF₆ gas in ranges from 0.1 MPa to 0.5 MPa were placed in a shielding box to reduce the external interference. The applied voltage was measured by a high voltage divider. The PD signal produced from the electrode systems was detected through a 50 Ω non-inductive resistor and analyzed by a digital storage oscilloscope (DSO) with a sampling rate of 5 GS/s and a DAQ system based on LabVIEW program.

In this thesis, the DIV was defined as the voltage at which discharge with magnitude over than 5 mV occurred at least one time per minute, and the DEV was defined as the voltage at which no discharge with magnitude over than 5 mV was observed when the applied voltage was gradually decreased from the PD onset voltage^{[5],[24]}. The DIV and DEV as a function of gas pressure, the maximum discharge magnitude (Q_{max}), the mean discharge magnitude (Q_{mean}), and pulse count in 5 seconds as a function of applied voltage as well as the statistical characteristics of each electrode system were analyzed.

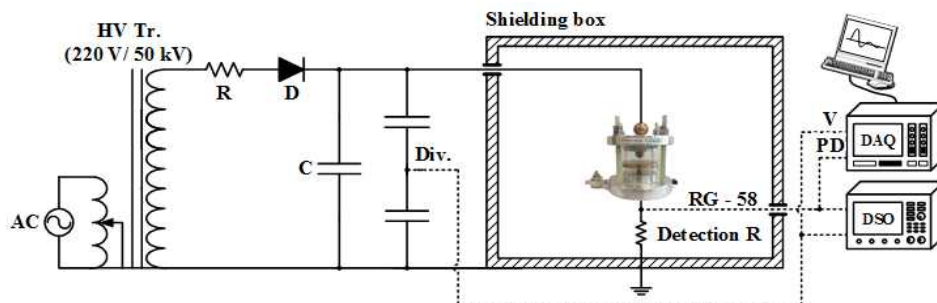
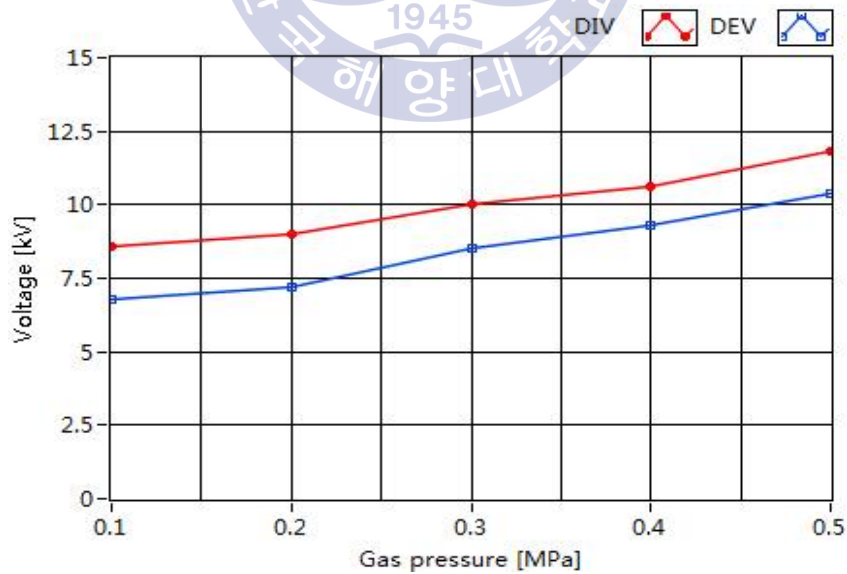


Fig. 3.4 Experimental setup

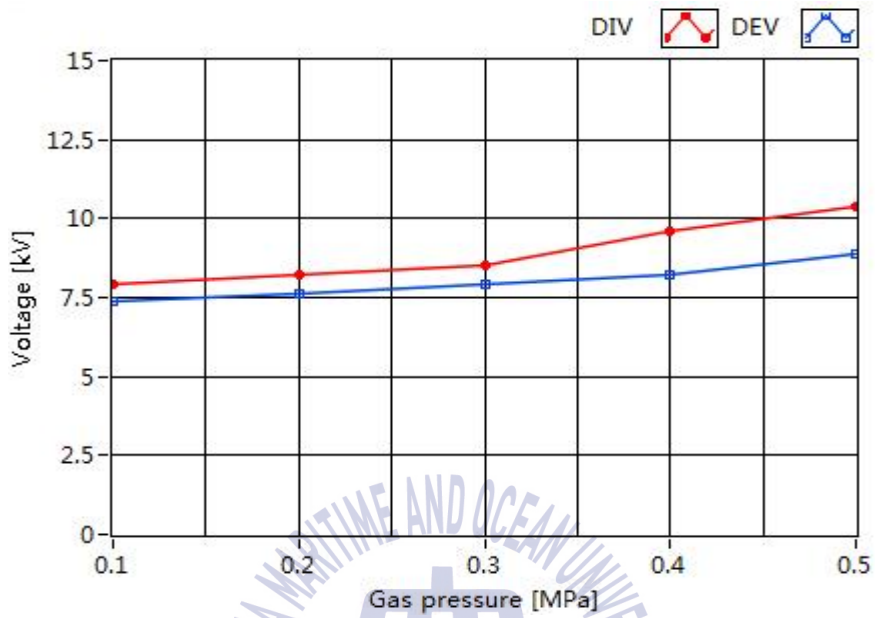
3.2 Results and Analysis

3.2.1 DIV and DEV

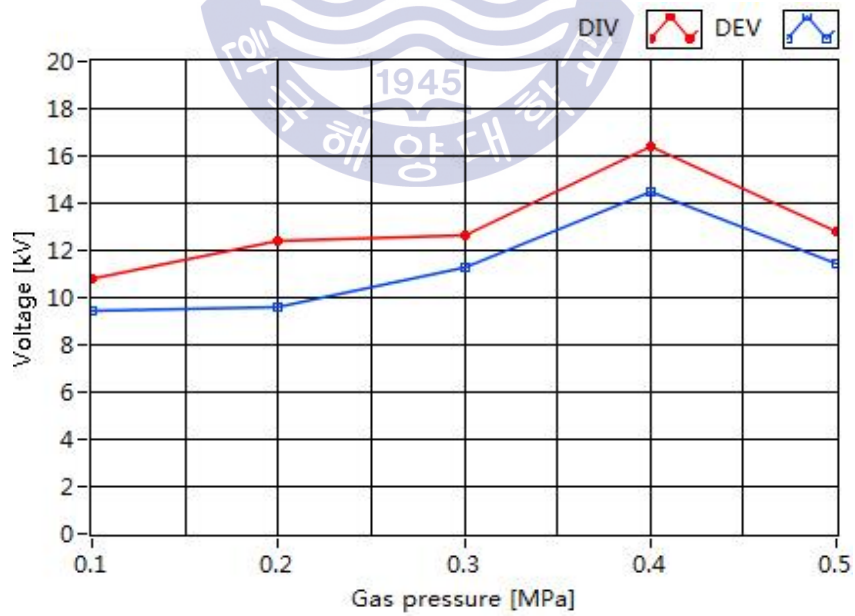
The DIV and DEV as a function of gas pressure of each electrode system are shown in Fig. 3.5. In POC, POE, and Crack, DIV and DEV increased as the gas pressure was raised. However, DIV in POC was somewhat higher than that in POE. It was due to the different mechanisms for generation of the starting electron. In POC, the starting electron is generated by photo-ionization while the starting electron in POE is generated by field emission from the cathode^{[24],[27]}. DIV and DEV in FP which were dependent on the position and state of particle on the plane electrode were not strongly affected by the gas pressure. Since the void was inside the epoxy insulator and there was no seeped SF₆ gas in the cavity, DIV and DEV in Void were almost similar with the increase of gas pressure.



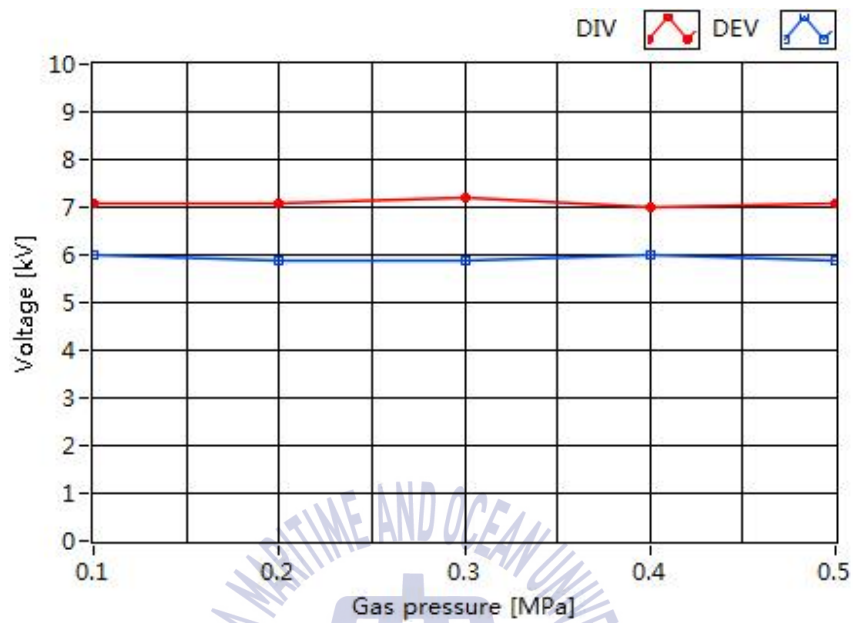
(a) POC



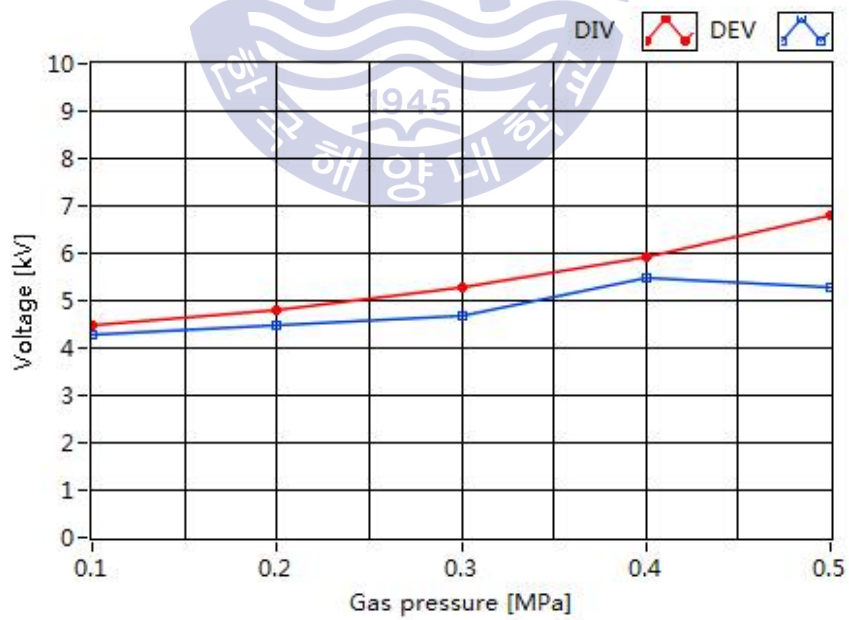
(b) POE



(c) FP



(d) Void



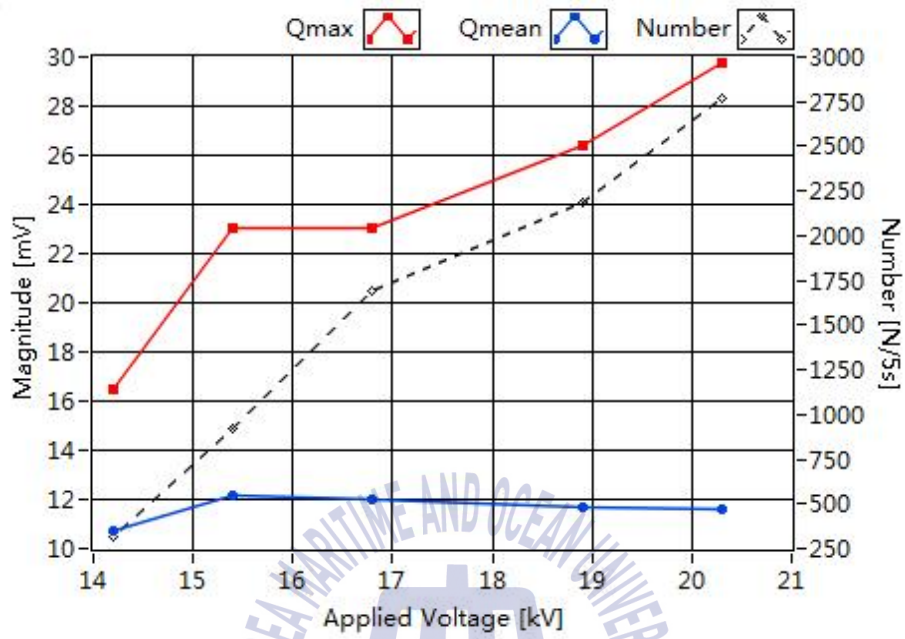
(e) Crack

Fig. 3.5 DIV and DEV as a function of gas pressure

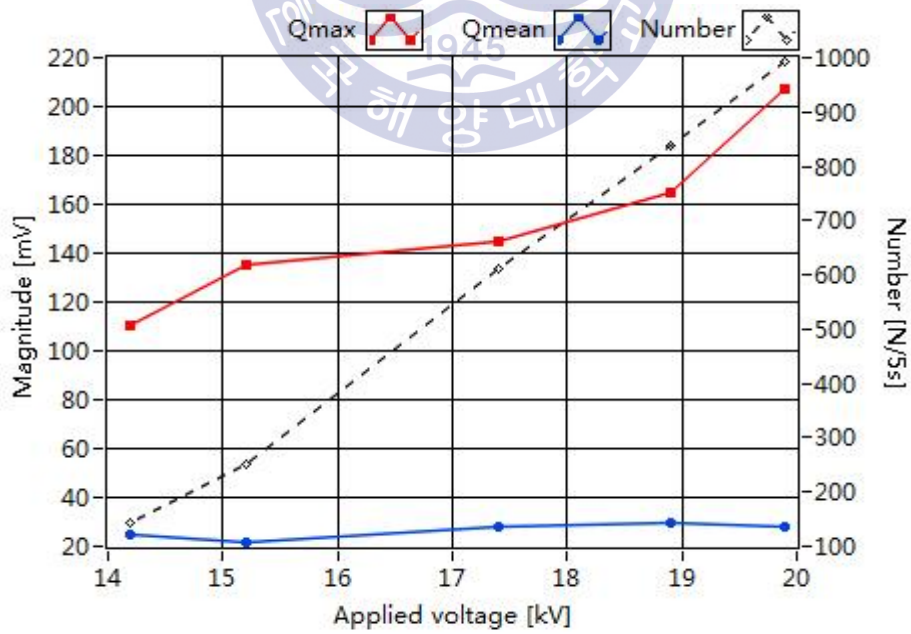
3.2.2 Discharge magnitude and pulse count

The maximum discharge magnitude Q_{max} , mean discharge magnitude Q_{mean} , and pulse count in 5 seconds as a function of applied voltage of each electrode system are shown in Fig. 3.6. For each electrode system, Q_{max} and pulse count increased as the applied voltage was raised. However Q_{mean} did not change greatly.

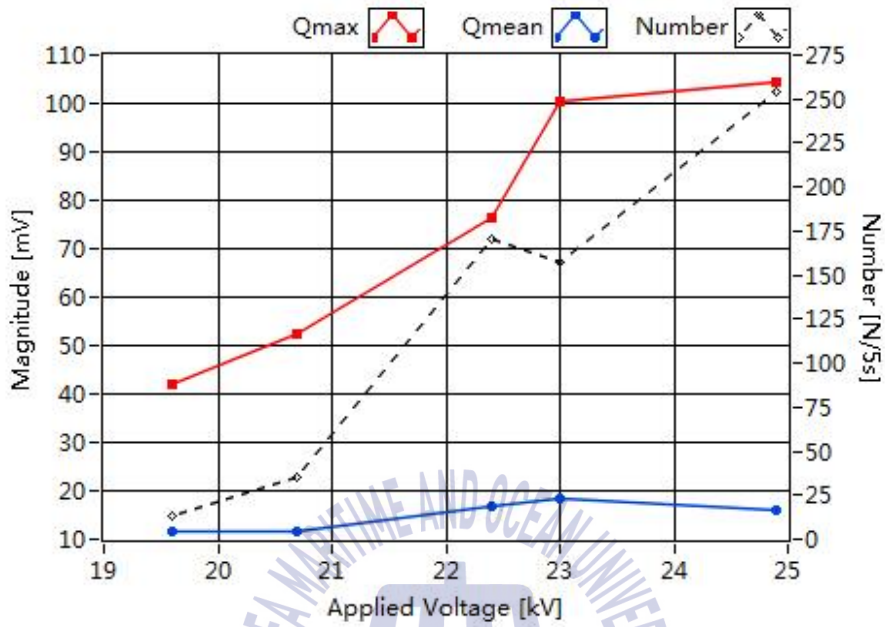
In POC, Q_{max} ranged from 16.48 mV to 29.77 mV when the applied voltage was raised from 14.2 kV to 20.3 kV and Q_{mean} were nearly 11.5 mV. The pulse count in 5 seconds increased from 317 to 2,771. Q_{max} range in POE as the voltage was increased from 14.2 kV to 19.9 kV was 110.38 ~ 207.54 mV and Q_{mean} were about 25 mV. The range of pulse count was 145 ~ 994. When the voltage applied to FP reached about 23 kV, the aluminum particle jumped in the electrode system. As a result, the pulse count increased rapidly and Q_{max} also increased from 42.05 mV before the particle jumping to 104.57 mV. In Void, the range of Q_{max} was 31.30 ~ 49.42 mV as the voltage was raised from 11.6 kV to 16.4 kV, the pulse count in 5 second increased from 104 to 1,190 and Q_{mean} were about 11.5 mV. When the voltage applied to Crack was raised from 11.5 kV to 17.5 kV, the range of Q_{max} and pulse count were 19.77 ~ 90.60 mV and 83 ~ 511, respectively. Q_{mean} in Crack increased linearly with the applied voltage.



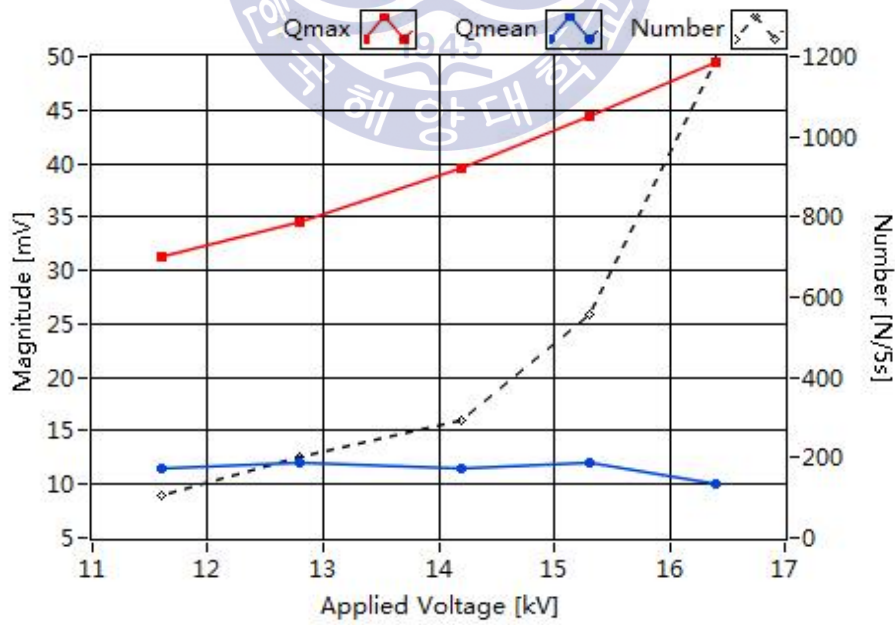
(a) POC



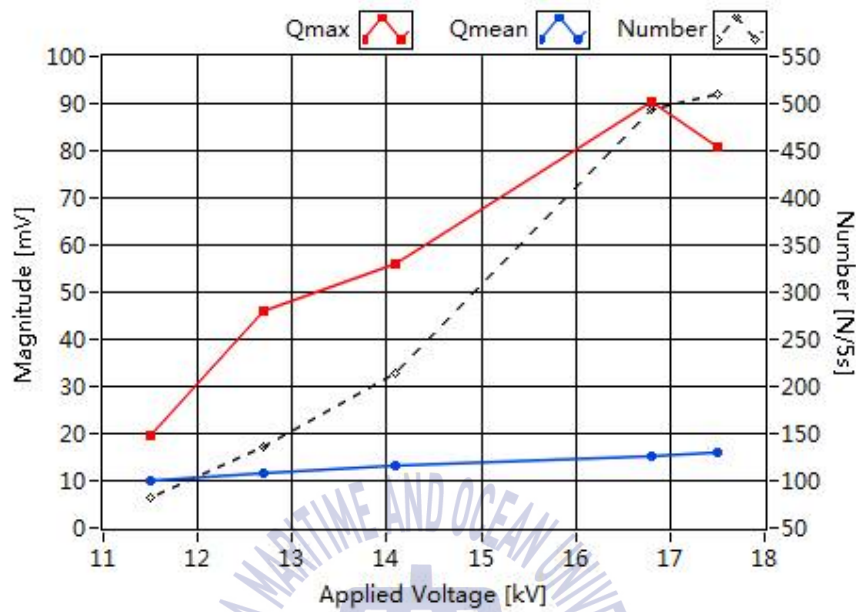
(b) POE



(c) FP



(d) Void



(e) Crack

Fig. 3.6 Discharge magnitude and pulse count as a function of applied voltage

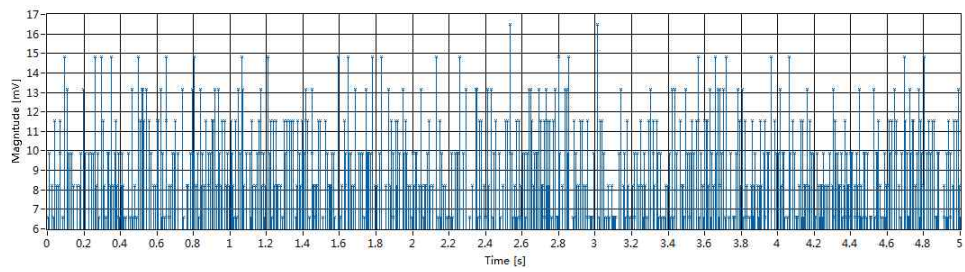
3.2.3 Statistical characteristics

The discharge distribution and density function such as TRPD, relation between discharge magnitude and time interval to its preceding discharge $q(\Delta t_{pre})$, relation between discharge magnitude and time interval to its successive discharge $q(\Delta t_{suc})$, density function of discharge magnitude $H(q)$, and density function of the time interval $H(\Delta t)$ of each electrode system are illustrated in Fig. 3.7 ~ 3.11. The distribution of statistical characteristics are shown in Fig. 3.12.

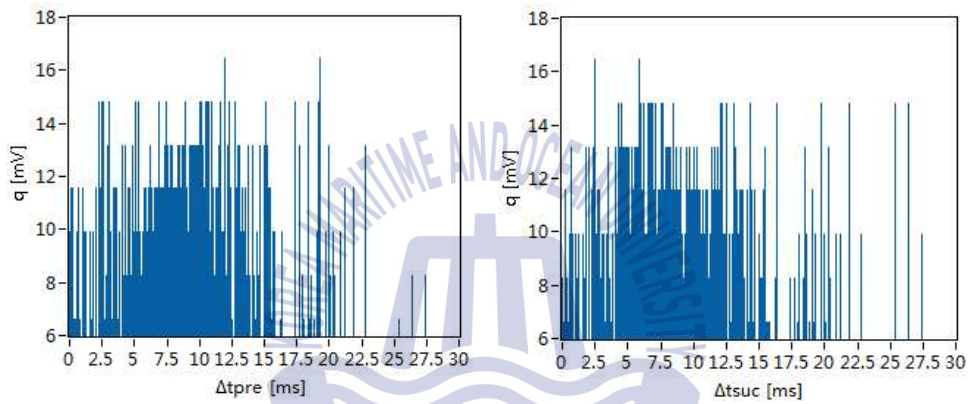
In POC, the peak value of $q(\Delta t_{pre})$ and $q(\Delta t_{suc})$ were the lowest compared to these of other four electrode systems. $H(q)$ of POC was scattered and was with high value of kurtosis. Since $H(\Delta t)$ of POC was almost symmetrical, it had a skewness value about 3. The peak value of $q(\Delta t_{pre})$ and $q(\Delta t_{suc})$ in

POE were highest compared to other four electrode systems. Also the statistical characteristics of $q(\Delta t_{pre})$ and $q(\Delta t_{suc})$ in POE were most widely distributed. In FP, the statistical characteristics of the discharge distribution and density function distributed in small range. In both Void and Crack, there was low similarity between $q(\Delta t_{pre})$ and $q(\Delta t_{suc})$. Also both of them had great value of skewness and kurtosis of $H(\Delta t)$ since the $H(\Delta t)$ were peaked with longer right tail. However, the statistical characteristics of $H(q)$ can be used to distinguish between Void and Crack. Therefore, it was verified that defects had different patterns and the defects identification algorithm for HVDC power facilities can be developed by the analysis of the statistical characteristics.



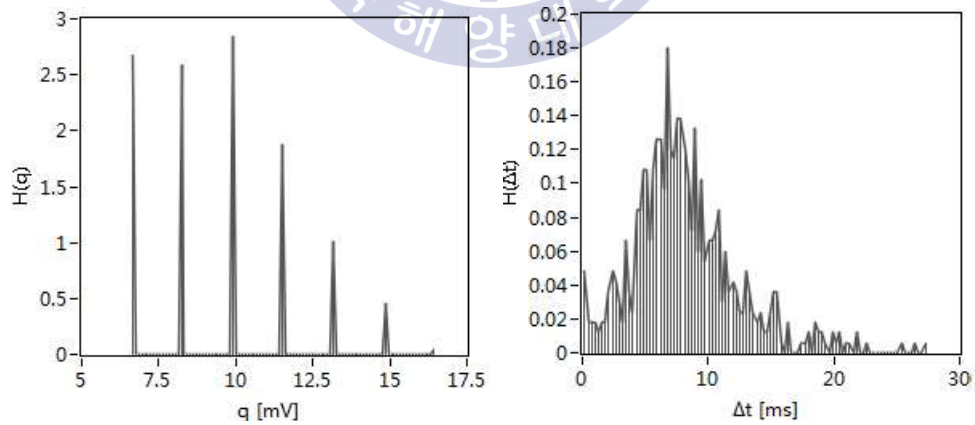


(a) TRPD



(b) $q(\Delta t_{pre})$

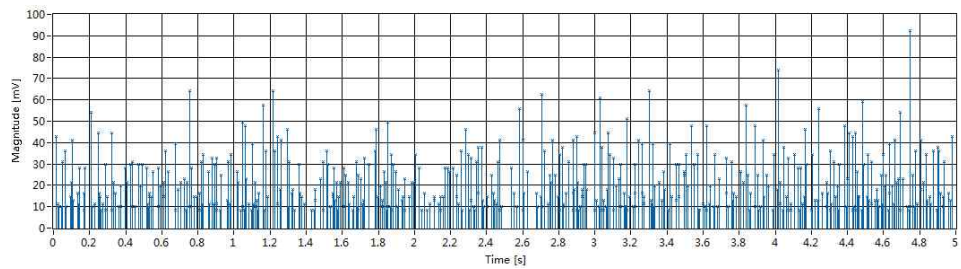
(c) $q(\Delta t_{suc})$



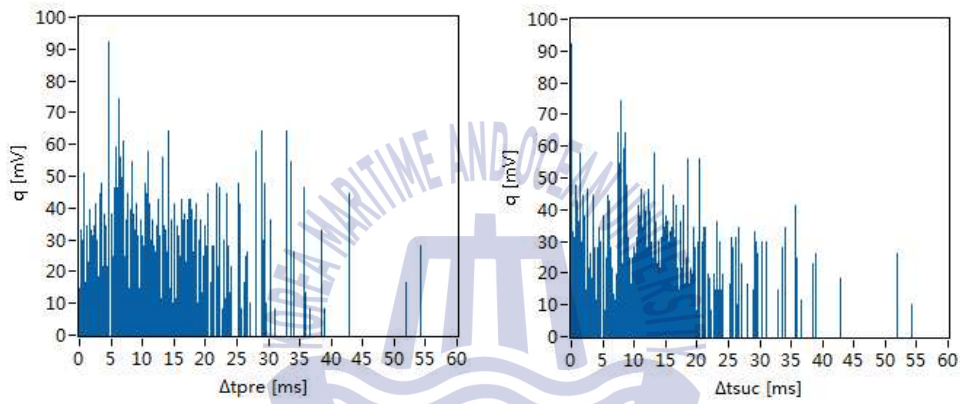
(d) $H(q)$

(e) $H(\Delta t)$

Fig. 3.7 Discharge distribution and density function of POC

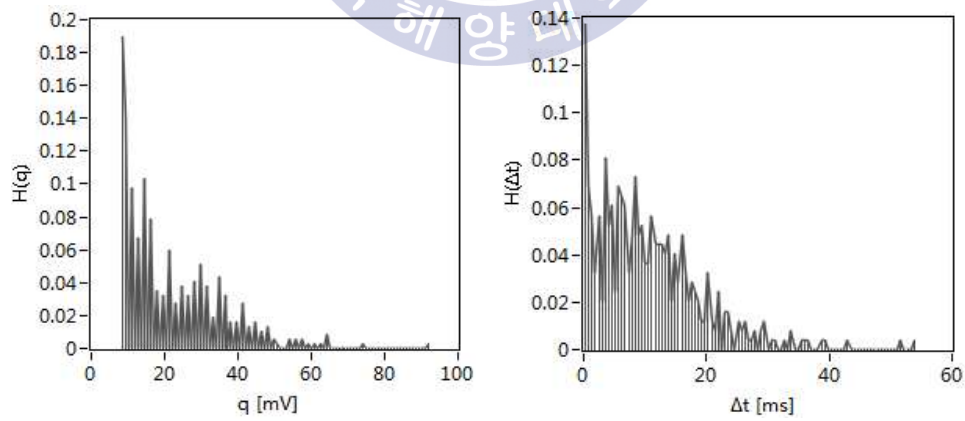


(a) TRPD



(b) $q(\Delta t_{pre})$

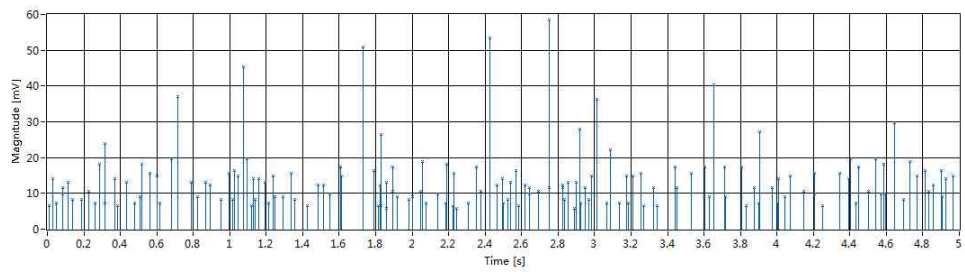
(c) $q(\Delta t_{suc})$



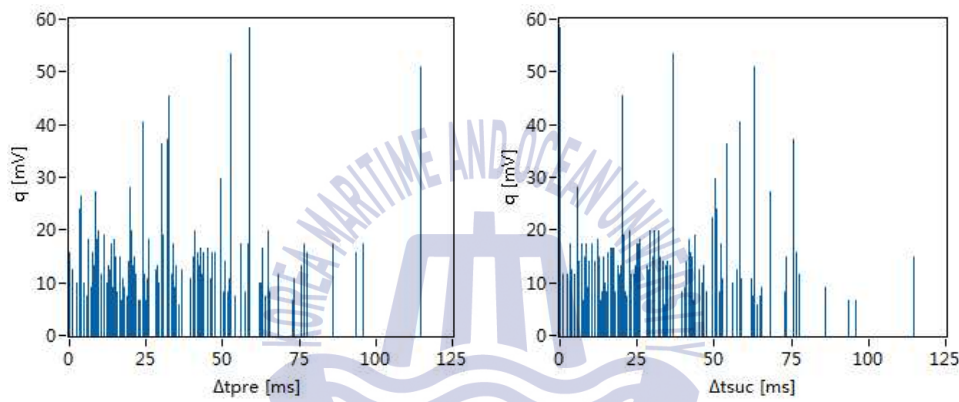
(d) $H(q)$

(e) $H(\Delta t)$

Fig. 3.8 Discharge distribution and density function of POE

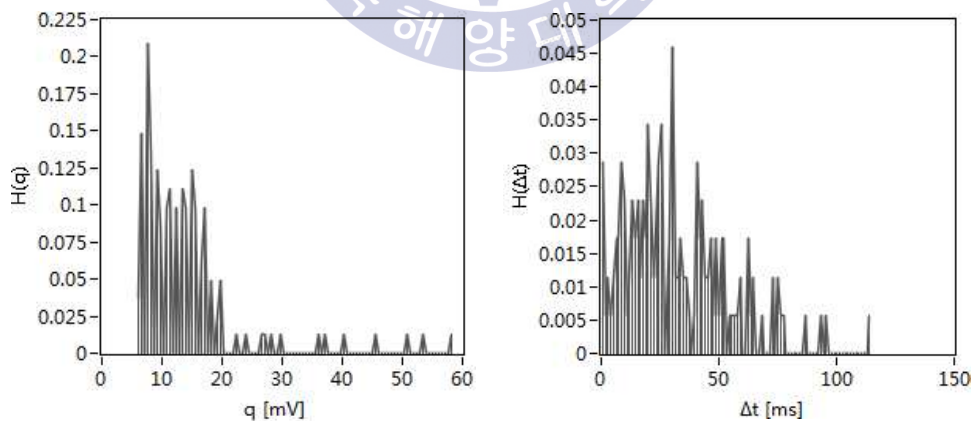


(a) TRPD



(b) $q(\Delta t_{pre})$

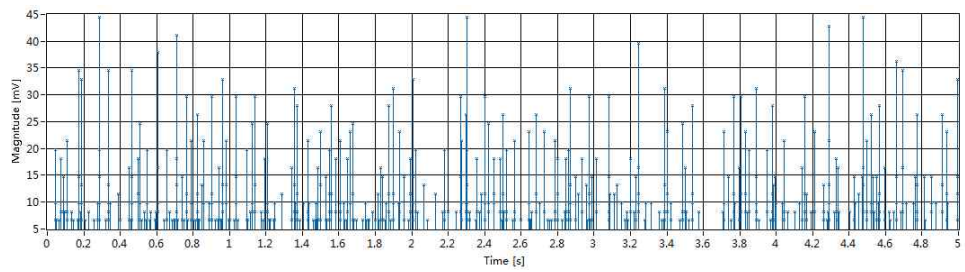
(c) $q(\Delta t_{suc})$



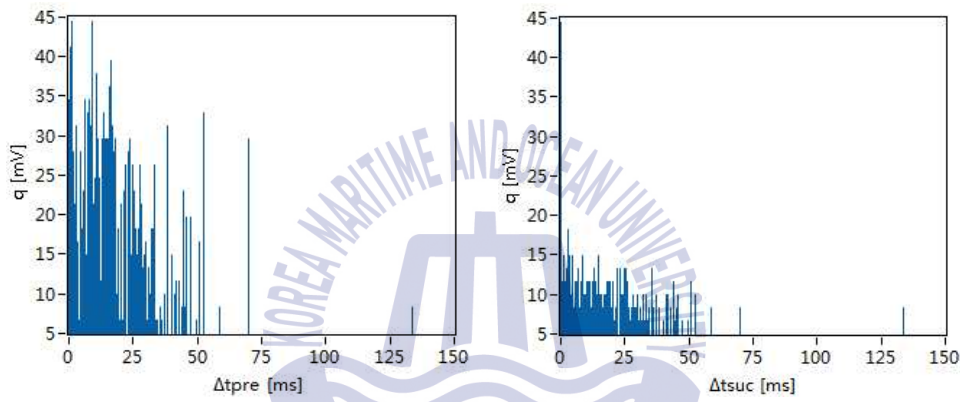
(d) $H(q)$

(e) $H(\Delta t)$

Fig. 3.9 Discharge distribution and density function of FP

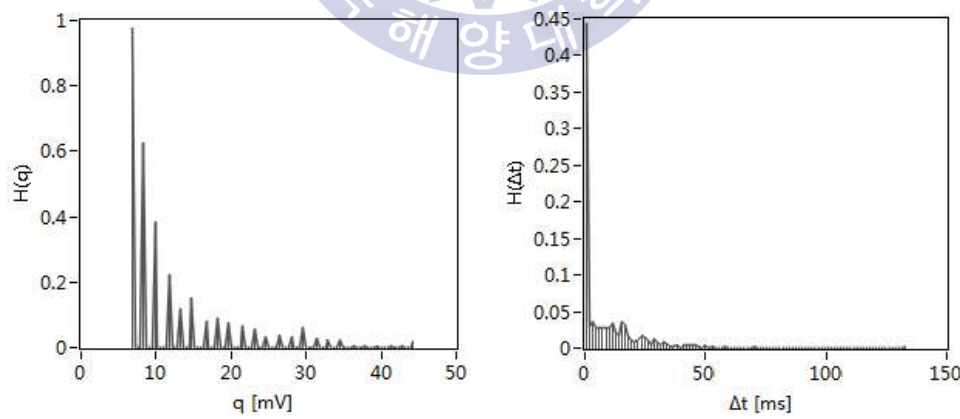


(a) TRPD



(b) $q(\Delta t_{pre})$

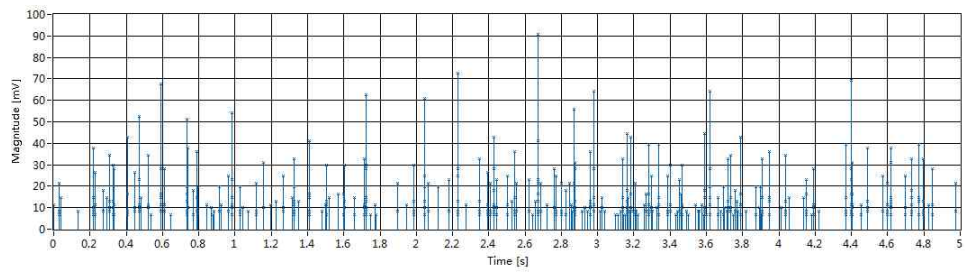
(c) $q(\Delta t_{suc})$



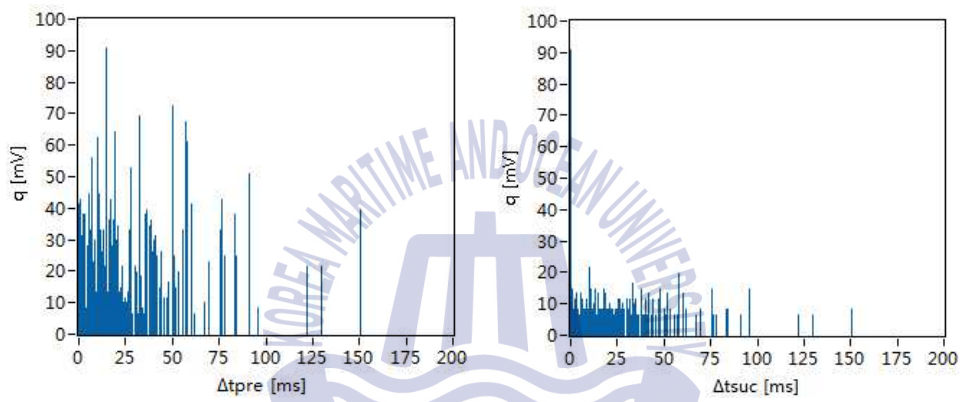
(d) $H(q)$

(e) $H(\Delta t)$

Fig. 3.10 Discharge distribution and density function of Void

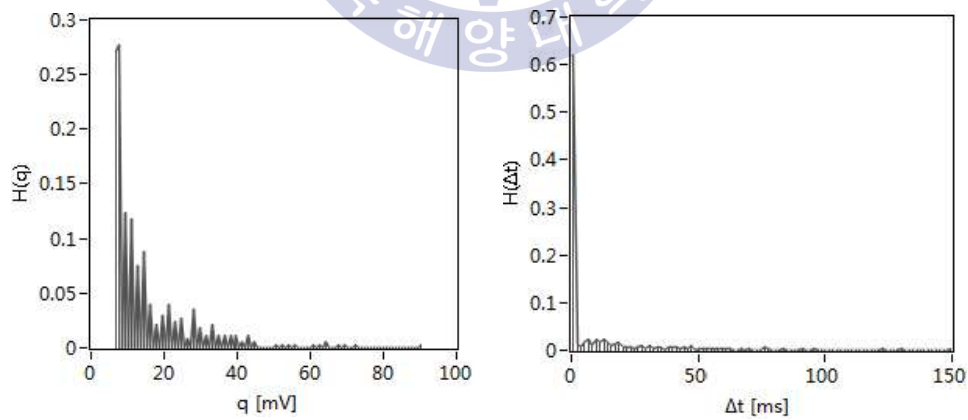


(a) TRPD



(b) $q(\Delta t_{pre})$

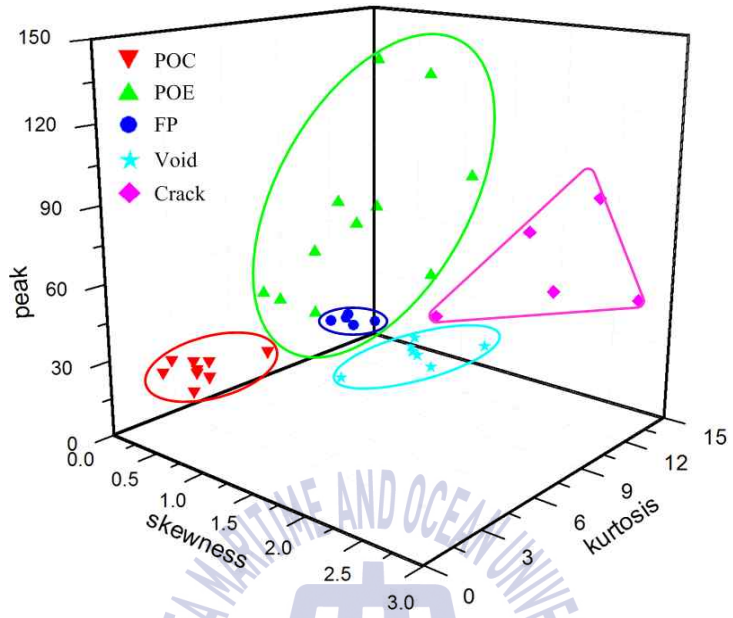
(c) $q(\Delta t_{suc})$



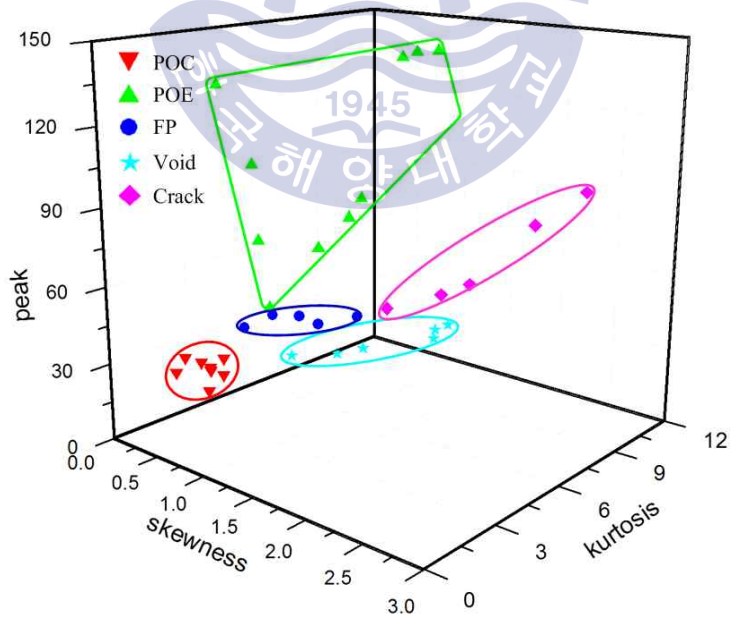
(d) $H(q)$

(e) $H(\Delta t)$

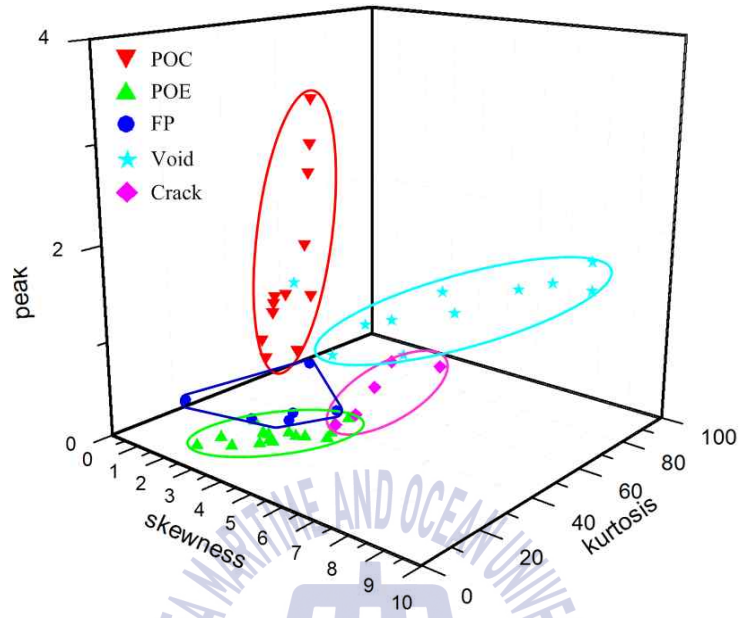
Fig. 3.11 Discharge distribution and density function of Crack



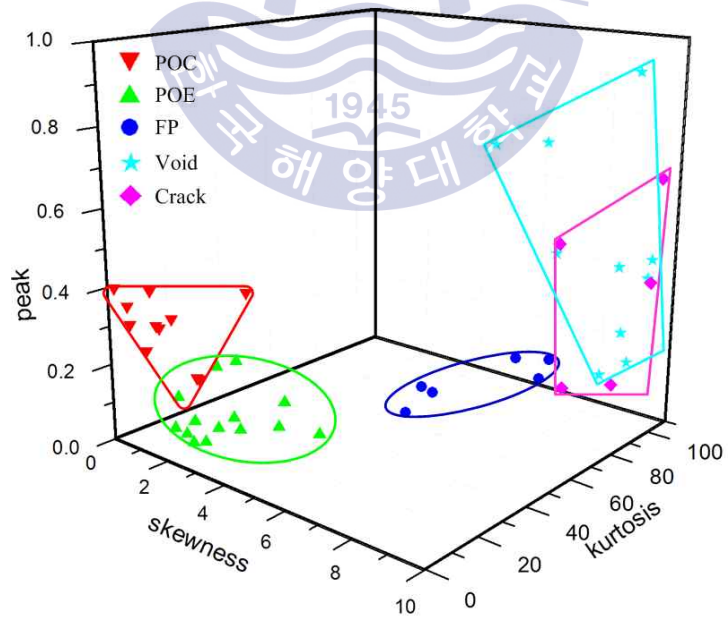
(a) $q(\Delta t_{pre})$



(b) $q(\Delta t_{suc})$



(c) $H(q)$



(d) $H(\Delta t)$

Fig. 3.12 Distribution of statistical characteristics

Chapter 4 Conclusions

This thesis dealt with the PD characteristics in SF₆ gas under HVDC on purpose of condition monitoring and diagnosis of gas insulated equipment operated under HVDC. Five types of electrode systems such as POC, POE, FP, Void, and Crack were fabricated to simulate typical insulation defects in GIS. Each electrode system was filled with SF₆ gas in ranges from 0.1 MPa to 0.5 MPa. The measurement system was developed based on RTOS by LabVIEW in which the PD pulse was measured and analyzed in real time within a specified period.

The DIV and DEV as a function of gas pressure, the discharge magnitude Q_{max} , Q_{mean} as well as pulse count as a function of applied voltage, the discharge distribution and density function such as TRPD, relation between discharge magnitude and time interval to its preceding discharge $q(\Delta t_{pre})$, relation between discharge magnitude and time interval to its successive discharge $q(\Delta t_{suc})$, density function of the discharge magnitude $H(q)$, and density function of the time interval $H(\Delta t)$ were investigated. Also the statistical characteristics such as skewness, kurtosis, and peak value of the discharge distribution and density function were analyzed.

The DIV and DEV in POC, POE, and Crack increased with the gas pressure while the DIV in POC were about 1 kV higher than that in POE. The gas pressure did not strongly affect the DIV and DEV in FP since they depended on the position and state of the particle on the plane electrode. The DIV and DEV in Void kept almost similar values of 7.1 kV and 6.0 kV with

the increase of the gas pressure, respectively.

In each electrode system, the maximum discharge magnitude Q_{max} and pulse count in 5 seconds increased as the applied voltage was raised. However, the mean discharge magnitude Q_{mean} did not change greatly.

The discharge distribution and density function of each electrode system presented distinguishable patterns, based on which it is possible to identify the type of defects in gas insulated equipment operated under HVDC. The defects identification algorithm such as centour score and artificial neural network method can be developed by analyzing the statistical characteristics such as skewness, kurtosis, and peak value extracted from the discharge distribution and density function^[28].



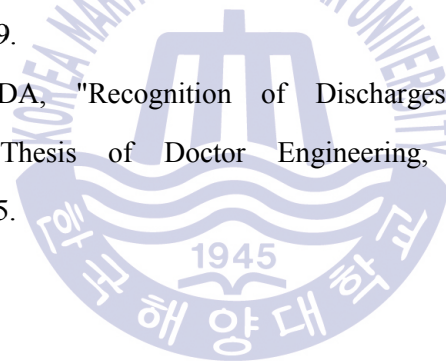
Reference

- [1] Roberto Rudervall, J.P. Charpentier, Raghuveer Sharma, "High Voltage Direct Current (HVDC) Transmission Systems Technology Review Paper", Energy Week 2000, 2000.
- [2] Yong-Joo Kim, "Road Map of HVDC Deployment in Korea", Electrical Insulation News in Asia Magazine, pp.31~32, 2010.
- [3] U. Schichler, M. Kuschel, J. Gorablenkow, "Partial Discharge Measurement on Gas Insulated HVDC Equipment", 18th International Symposium on High Voltage Engineering, pp.2,313~2,316, 2013.
- [4] N. H. Malik, A. A. Al-Arainy, M. I. Qureshi, "Electrical Insulation in Power System", Riyadh, 1998.
- [5] IEC International Standard 60270, "High Voltage Test techniques - Partial Discharge Measurements", 2000.
- [6] Sacha M. Markalous, Stefan Tenbohlen, Kurt Feser, "Detection and Location of Partial Discharges in Power Transformers using Acoustic and Electromagnetic Signals", IEEE Transactions on Dielectrics and Electrical Insulation, Vol. 15, pp.1,576~1,583, 2008.
- [7] Dr F. H. Kreuger, "Partial Discharge Detection in High Voltage Equipment", Butterworth, pp.15~35, 1989.
- [8] 趙智大, "高電壓技術", 中國電力出版社, pp.83~87, 2006.
- [9] Roland Piccin, "Partial Discharge Analysis in HVDC Gas Insulated Substations", Thesis Project, Delft University of Technology, 2013.
- [10] Peter H. F. Morshuis, Johan J. Smit, "Partial Discharges at dc Voltage:

- Their Mechanism, Detection and Analysis", IEEE Transactions on Dielectrics and Electrical Insulation Vol. 12, No. 2, pp.328~340, 2005.
- [11] U. Fromm, "Interpretation of Partial Discharges at dc Voltages", IEEE Transactions on Dielectrics and Electrical Insulation Vol. 2, No. 5, pp.761~770, 1995.
- [12] Su SU Win, Sebastian Coenen, Stefan Tenbohlen, "Partial Discharge Localization in Power Transformer", 18th International Symposium on High Voltage Engineering, pp.781~786, 2013.
- [13] Rosmaini Ahmad, Shahrul Kamaruddin, "An Overview of Time-based and Condition-based Maintenance in Industrial Application", Computers and Industrial Engineering, Vol. 63, No. 1, pp.135~149, 2012.
- [14] IEEE Std C57.127, "IEEE Guide for the Detection and Location of Acoustic Emissions form PD in Oil-Immersed Power Transformers and Reactors", IEEE, 2007.
- [15] Gyung-Suk Kil, Il-Kwon Kim, Dae-Won Park, Su-Yeon Choi, Chan-Yong Park, "Measurements and Analysis of Acoustic Signals Produced by Partial Discharge in Insulation oil", Current Applied Physics, Vol. 9, No. 2, pp.296~300, 2009.
- [16] Martin D. Judd, Li Yang, Ian B. B. Hunter, "Partial Discharge Monitoring for Power Transformers Using UHF Sensors Part 1: Sensors and Signal Interpretation", IEEE Electrical Insulation Magazine, Vol. 21, No. 2, pp.5~14, 2005.
- [17] Martin D. Judd, Li Yang, Ian B. B. Hunter, "Partial Discharge Monitoring for Power Transformers Using UHF Sensors Part 2: Field Experience", IEEE Electrical Insulation Magazine, Vol. 21, No. 3,

- pp.5~13, 2005.
- [18] IEC International Standard 60599, "Mineral Oil-impregnated Electrical Equipment in Service - Guide to the Interpretation of Dissolved and Free Gases Analysis", 2007.
- [19] A. Cavallini, A. Contin, Gian Carlo Montanari, F. Puletti, "Advanced PD Inference in On-Field Measurements. I. Noise rejection", IEEE Transactions on Dielectrics and Electrical Insulation, Vol. 10, No. 2, pp.216~224, 2003.
- [20] Si Wenrong, Li Junhao, Yuan Peng, Li Yanming, "Digital Detection, Grouping and Classification of Partial Discharge Signals at DC Voltage", IEEE Transactions on Dielectrics and Electrical Insulation, Vol. 15, No. 6, pp.1,663~1,674, 2008.
- [21] Andrea Cavallini, Gian Carlo Montanari, Marco Tozzi, Xiaolin Chen, "Diagnostic of HVDC Systems Using Partial Discharges", IEEE Transactions on Dielectrics and Electrical Insulation Vol. 18, No. 1, pp.275~284, 2011.
- [22] Peter Morshuis, Marc Jeroense, Jens Beyer, "Partial Discharge Part XXIV: Analysis of PD in HVDC Equipment", IEEE Electrical Insulation Magazine, Vol. 13, No. 2, pp.6~16, 1997.
- [23] G. Hoogenraad, P. H. F. Morshuis, C. Petrarca, "Classification of Partial Discharges for DC Equipment", IEEE Annual Report of Conference on Electrical Insulation and Dielectric Phenomena, Vol. 1, No. 1, pp.110~112, 1996.
- [24] Roland Piccin, Armando Rodrigo Mor, Peter Morshuis, Alain Girodet, Johan Smit, "Partial Discharge Analysis of Gas Insulated Systems at High

- Voltage AC and DC", IEEE Electrical Insulation Magazine, Vol. 22, No. 1, pp.218~227, 2015.
- [25] Serge Blufpand, "Partial Discharge Recognition of Defects in Gas Insulated Systems under DC Voltage", Thesis of Master Engineering, Delft University of Technology, 2014.
- [26] G. Hoogenraad. J. Beyer, "Digital HVDC Partial Discharge Testing", IEEE International Symposium on Electrical Insulation, pp.448~451, 2000.
- [27] N. H. Malik, A. H. Qureshi, "The Influence of Voltage Polarity and Field Non-Uniformity on the Breakdown Behavior of Rod-Plane Gaps Filled with SF₆", IEEE Transactions on Electrical Insulation, Vol. 14, No. 6, pp.327~333, 1979.
- [28] Andrej KRIVDA, "Recognition of Discharges: Discrimination and Classification", Thesis of Doctor Engineering, Delft University of Technology, 1995.



Published Paper

◎ Proceedings of domestic conference

- [1] Gi-Woo Jeong, Sun-Jae Kim, Guoming Wang, Gyung-Suk Kil, “Design and Fabrication of On-Line Lightning Arrester Analyzer for Traction”, Proceedings of the 2014 Spring Conference of the Korean Society for Railway, pp.145.1-145.5, 2014.
- [2] Sun-Jae Kim, Gi-Woo Jeong, Guoming Wang, Gyung-Suk Kil, “Seasonal Variation of Ground Impedance for a Copper-rods and a Carbon-block”, Proceedings of the 2014 Spring Conference of the Korean Society for Railway, pp.147.1-147.6, 2014.
- [3] Hee-Ju Ha, Hyang-Eun, Jo, Guoming Wang, Gyung-Suk Kil, Byung-Gwon Choi, “Operation Characteristics of LEDs at Ultra-low Temperature”, Proceedings of the 38th The Korean Society of Marine Engineering Spring Conference, pp.123, 2014.
- [4] Guoming Wang, Sun-JaeKim, Hee-Ju Ha, Kyoung-Soo Park, “Operating Characteristics of LED Bulbs at Ultra Low Temperature”, Proceedings of the 38th the Korean Society of Marine Engineering Fall Conference, p.125, 2014.
- [5] Sun-Jae Kim, Jin-Wook Kim, Gi-Woo Jeong, Guoming Wang, Gyung-Suk Kil, “Design and Fabrication of a LED Working Light for Vessels”, Proceedings of the 38th the Korean Society of Marine Engineering Fall Conference, p.121, 2014.

- [6] Guoming Wang, Sun-Jae Kim, Hyang-Eun, Jo, Min-Young Yun, Gyung-Suk Kil, “Partial Discharge Characteristics in SF₆ Gas under HVDC”, Proceedings of the Korean Institute of Electrical and Electronic Material Engineers Annual Autumn Conference, p.91, 2014.
- [7] Hyang-Eun, Jo, Sun-Jae Kim, Guoming Wang, Gyung-Suk Kil, “Analysis of Partial Discharge Characteristics under AC and DC in SF₆ Gas”, Proceedings of the 2015 Spring Conference of the Korean Society for Railway, KSR2015S306, 2015.



© **Proceedings of international conference**

- [1] Jin-Wook Kim, Se-Jin Kim, Sun-Jae Kim, Guoming Wang, Gyung-Suk Kil, “Development of the LED Searchlight for Vessels”, Proceedings of the International Conference on Electrical Engineering, pp.1,914-1,919, Korea, 2014.
- [2] Guoming Wang, Hyang-Eun, Jo, Sun-Jae Kim, Gyung-Suk Kil, “Comparison of Partial Discharge Pulse Waveforms Between AC and DC Voltages in SF₆ Gas”, Proceedings of the International Conference on Electrical Engineering, Hong Kong, 2015.
- [3] Jin-Wook Kim, Guoming Wang, Min-Young Yun, Gyung-Suk Kil, “A Condensing Technology for a LED Searchlight”, Proceedings of The International Conference on Electrical Engineering, Hong Kong, 2015.
- [4] Guoming Wang, Sun-Jae Kim, Hyang-Eun Jo, Gyung-Suk Kil, Sung-Wook Kim, “Partial Discharge Localization in Insulation Oil by Electrical-Acoustic Method”, Proceedings of the 19th International Symposium on High Voltage Engineering, Czech Republic, 2015.
- [5] Guoming Wang, Sun-Jae Kim, Hyang-Eun Jo, Gi-Woo Jeong, Gyung-Suk Kil, “Algorithm for Defects Identification by Analysis of PD Pulses in SF₆ Gas”, Proceedings of the 19th International Symposium on High Voltage Engineering, Czech Republic, 2015.
- [6] Hyang-Eun Jo, Sun-Jae Kim, Guoming Wang, Sung-Wook Kim, “Analysis of DIV and DEV in SF₆-N₂ Mixture Gas”, Proceedings of the 19th International Symposium on High Voltage Engineering, Czech Republic, 2015.

Acknowledgments

It has been nearly two years since I started my master course in Korea. I would like to express my sincere gratitude to everyone who helped and inspired me. Thanks to everyone, I enjoyed my life in Korea.

First and foremost, I would like to express the deepest appreciation to my supervisor Prof. Gyung-Suk Kil, who gave me a precious opportunity to continue my studies and truly changed my life. It is his expertise as well as his attitude to work and life that encourage me and influence me. I am so fortunate to study under his instruction and to enrich my knowledge and experience with his support. I am also grateful to Prof. Yoon-Sik Kim, Prof. Nakwon Jang, Prof. Sung-Geun Lee, Prof. Tae-In Jeon, Prof. Dong-Hoan Seo, and Prof. Yang-Ick Joo for their kind guidance and insightful comments on my thesis.

I would like to thank members in Applied High Voltage Laboratory for their help and understanding. Thanks to laboratory leader Mr. Sun-Jae Kim, who always carefully manages our laboratory and gave valuable suggestions for my thesis. Thanks to doctor candidate Miss. Hyang-Eun Jo for her advices during the modification. I am thankful to Mr. Tae-Seong Kim for his kind concern about my daily life and to Mr. Min-Young Yun for his help. My thanks also goes to Mr. Seo-Jun Park and Mr. Kyoung-Soo Park, with whom I accomplished the experiment. As well as Jang-Hoon Lee, welcome to join our laboratory.

I also wish to express my sincere thanks to all of the seniors graduated from our laboratory for their guidance on knowledge and getting along with others, especially to Dr. Dae-Won Park, M. Eng. Min-Su Kim, M. Eng. Se-Jin Kim, M. Eng. Hee-Ju Ha, M. Eng. Gi-Woo Jeong and M. Eng. Jin-Wook Kim, who have lived together with me in laboratory. As well as part-time doctor and master candidate Mr. Sung-Wook Kim, Mr. Hong-Keun Ji, Mr. Jung-Yoon Lee and Mr. Sung-Hwan Byun, it is my great pleasure to study with you in the same laboratory.

Last but not least, I would like to express my gratitude to my parents for giving birth to me and bringing me up.

In a word, I am sincerely grateful to all the people who have helped and encouraged me along the way.

Sincerely
Guoming Wang